intervals and $A(\infty)$ was the peak intensity at $t = \infty$, was the observed first-order rate constant. Second-order rate constants were calculated by use of the appropriate form of the McKay equation (eq 12) and are listed in Table V.

Kinetics of the Reaction of Cp_2ZrMe_2 with $CpM(CO)_3H$ (M = W, Mo, Cr). Solutions of $CpM(CO)_3H$ and Cp_2ZrMe_2 in THF/0.5% benzene (or CD_3CN/0.5% benzene) were prepared and mixed under an inert atmosphere so that at least a tenfold excess (0.55-2.34 M) of the more plentiful reagent resulted (see Tables VI and VII). Because of the rapid reaction of Cp_2ZrMe_2 with $CpM(CO)_3H$ (M = Mo, Cr) in CD_3CN, it was necessary to add the solutions of these metal hydrides to a frozen solution of Cp_2ZrMe_2. All reaction mixtures were placed in NMR tubes, frozen and degassed several times, and then sealed under vacuum.

Kinetic runs at -6 °C and above were performed in constant temperature baths thermostatically controlled within ±0.1 or 0.2 °C. Samples were removed from the bath at appropriate intervals and quenched in liquid nitrogen. The NMR probe was cooled to 30 °C or more below the reaction temperature to prevent significant reaction while sampling. For reactions run at -6 °C or below, the reaction was run directly in the NMR probe. The sampling time corresponding to a particular point was then taken as the mean reaction time during the series of pulses required to collect that spectrum. In all cases the extent of reaction was determined by comparing peak heights of starting materials and products with that of an internal standard (benzene). Relative peak widths at half-height were routinely checked to ensure the validity of this procedure.

In most cases the peaks monitored were those of Cp ligands. However, when $CpCr(CO)_3H$ was a reactant, its Cp peak was broadened by the exchange of $CpCr(CO)_3^-$ units with the product. The extent of disappearance of $CpCr(CO)_3H$ was therefore determined from the decrease in height of its hydride peak. (The hydride chemical shift is unaffected by the exchange process and the hydride resonance therefore does not broaden.) In one case with near-equal concentrations of $CpCr(CO)_3H$ and Cp_2ZrMe_2 (the fourth run from the bottom in Table VII), the progress of the reaction was determined by monitoring the disappearance of Cp_2ZrMe_2.

The standard deviations of extrapolated rate constants were calculated from the standard deviations and covariance of $\Delta H^{\ddagger}$ and $\Delta S^{\ddagger}$.[1a]

Acknowledgment. This research was supported by NSF Grant CHE85-16415. We are grateful to Colonial Metals, Inc., for a donation of OsO_4, to Prof. Walter Klemperer for advice on measuring the rate of deprotonation of $HRe(CO)_5$, and to Prof. E. L. King for helpful discussions on the extraction of rate constants from the rate of approach to isotopic equilibrium.

Stereochemically Nonrigid Tungsten Alkylidene Complexes. Barriers to Rotation about the Tungsten to Carbon Double Bond

Jacky Kress and John A. Osborn*

Contribution from the Laboratoire de Chimie des Métaux de Transition et de Catalyse, U.A. au C.N.R.S. No. 424, Institut Le Bel, Université Louis Pasteur 4, 67000 Strasbourg, France.
Received August 27, 1986

Abstract: The tungsten alkylidene complexes $W(CHR)(OCH_2\text{-}t\text{-}Bu)_2Br_2$ [R = *n*-Bu (**4**), *sec*-Bu (**5**), Ph (**6**)], $W[\overline{C\text{-}(CH_2)_3CH_2}](OCH_2\text{-}t\text{-}Bu)_2Br_2$ (**7**), $W(\overline{CH\text{-}t\text{-}Bu})(OCH_2\text{-}t\text{-}Bu)_3X$ [X = Cl (**8**), Br (**9**), I (**10**)], $W(CHR)(OCH_2\text{-}t\text{-}Bu)_3Br$ [R = *n*-Bu (**11**), *sec*-Bu (**12**), Ph (**13**)], $W[\overline{C(CH_2)_3CH_2}](OCH_2\text{-}t\text{-}Bu)_3Br$ (**14**), and $W(CH\text{-}t\text{-}Bu)(OCH_2\text{-}t\text{-}Bu)_4$ (**15**) have been synthesized and studied by variable-temperature ^1H NMR spectroscopy. The low temperature limiting spectra observed for all these compounds (except for **15**) are consistent with a formal trigonal-bipyramidal arrangement of the five ligands around the tungsten. The carbene ligand occupies an equatorial position with its substituents lying in the trigonal plane. Notably the two diastereomers expected for **12** could be distinguished. At higher temperature, compounds **8-14**, but not compounds **4-7**, appear to undergo two distinct intramolecular dynamic processes. The lower energy process ($12.3 < \Delta G^{\ddagger} < 15.7$ kcal·mol^{-1}) consists of a simple carbene ligand rotation about the tungsten-carbon double bond. Its barrier is strongly dependent on the π-donor character of the ligands in the axial position of the bipyramid. Strong donors destabilize the ground state of these molecules by the resultant electronic repulsion created between the lone pairs of the π-donor ligand and the $(d_{xz}\text{-}p_z)$ π electrons of the metal-carbene π-bond. Since the orthogonal orientation of the carbene ligand is energetically largely unaffected by axial donation, the rotational barrier is thereby lowered. The higher energy process ($15.3 < \Delta G^{\ddagger} < 18.9$ kcal·mol^{-1}) consists of scrambling of all three neopentoxo groups, but it is not specific to carbene complexes. The particular behavior shown by compounds **15** and $[W(CH\text{-}t\text{-}Bu)(OCH_2\text{-}t\text{-}Bu)_3]^+Ga_2Br_7^-$ (**16**) is also discussed.

Transition-metal carbene complexes are generally recognized as important reactive intermediates in organometallic chemistry, in particular in certain catalytic reactions, e.g., olefin metathesis[1] and the Fischer-Tropsch synthesis.[2] The nature of the metal-carbon bonding interaction is thus of fundamental interest, and several theoretical studies have been carried out in attempts to evaluate its strength as well as the barrier to rotation about the expected metal-carbon double bond.[3] If structural studies on stable species show that metal-carbon bond lengths are effectively consistent with a double bonding interaction between the metal and the carbene fragment,[4] experimental studies on the rotational barrier are surprisingly limited in number, despite the numerous carbene complexes that have been synthesized in recent years. The only neutral high oxidation state complexes for which these barriers were determined experimentally are thus compounds MCp(CHR)X (M = Ta, Nb), in which the carbene-ligand rotation was found to be largely dependent on steric effects.[5]

Apart from these fundamental considerations, such barriers to carbene rotation, as well as the activation energies of other dynamic processes in carbene complexes, can have moreover important potential implications in chemical reactivity. For example,

(1) Ivin, K. J. *Olefin Metathesis*; Academic Press: London 1983.
(2) Muetterties, E. L. *J. Organomet. Chem.* **1980**, *200*, 177.
(3) (a) Lauer, J. W.; Hoffmann, R. *J. Am. Chem. Soc.* **1976**, *98*, 1729. (b) Schilling, B. E.; Hoffmann, R.; Lichtenberger, D. L. *Ibid.* **1979**, *101*, 585. (c) Rappé, A. K.; Goddard, W. A., III *Ibid.* **1980**, *102*, 5114. (d) Spangler, D.; Wendoloski, J. J.; Dupuis, M.; Chen, M. M. L.; Schaeffer, H. F., III *Ibid.* **1981**, *103*, 3987. (e) Nakamura, S.; Dedieu, A. *Nouv. J. Chim.* **1982**, *6*, 23. (f) Kostic, N. M.; Fenske, R. F. *J. Am. Chem. Soc.* **1982**, *104*, 3879. (g) Nakatsuji, H.; Ushio, J.; Han, S.; Yonezawa, T *Ibid.* **1983**, *105*, 426. (h) Taylor, T. E.; Hall, M. B. *Ibid.* **1984**, *106*, 1576. (i) Ushio, J.; Nakatsuji, H.; Yonezawa, T. *Ibid.* **1984**, *106*, 5892. (j) Marynick, D. S.; Kirkpatrick, C. M. *Ibid.* **1985**, *107*, 1993. (k) Gregory, A. R.; Mintz, E. A. *Ibid.* **1985**, *107*, 2179.
(4) See for instance: Casey, C. P.; Burkhardt, T. J.; Bunnell, C. A.; Calabrese, J. C. *J. Am. Chem. Soc.* **1977**, *99*, 2127. Churchill, M. R.; Missert, J. R.; Youngs, W. J. *Inorg. Chem.* **1981**, *20*, 3388.
(5) Schrock, R. R.; Messerle, L. W.; Wood, C. D.; Guggenberger, L. J. *J. Am. Chem. Soc.* **1978**, *100*, 3793.

0002-7863/87/1509-3953$01.50/0

Scheme I

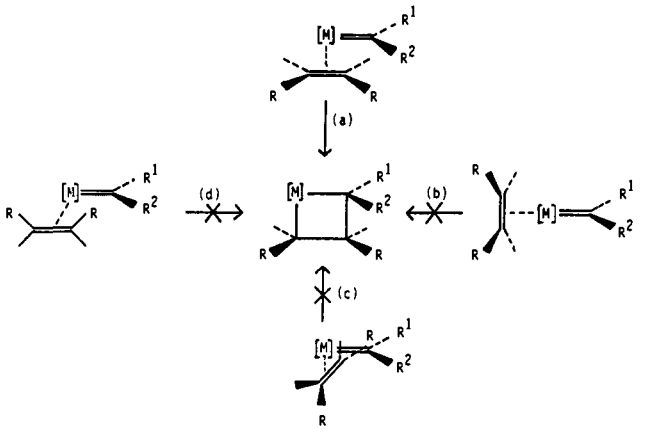

Scheme II

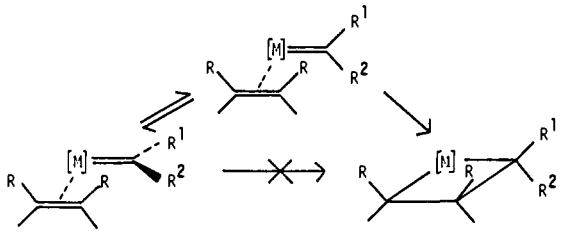

one important condition for a metal carbene complex to be an efficient catalyst for the metathesis of olefins lies in the facile generation of a metallacyclobutane intermediate through the [2 + 2] addition of the carbon–carbon π bond of the olefin across the metal–carbon π bond of the complex[1] (Scheme Ia).

Such a reaction will seemingly not take place if the olefin approaches the metal–carbene complex (whether or not an intermediate π-complex is formed) (i) in a position which is not cis to the metal–carbene binding site (Scheme Ib), (ii) with its C=C axis not aligned with the M=C axis (Scheme Ic), or (iii) with its molecular plane not parallel to that of the carbene group (Scheme Id). In the case of Scheme Id however, metallacycle formation can still take place if a prior 90° rotation of the carbene ligand about the M=C bond can be achieved (Scheme II).

We believed that the activation energy of such a process could become rate determining and that such a barrier may thus be responsible for the reduced catalytic activity for olefin metathesis of many of the group VI carbene complexes as yet isolated.[1]

Compounds $W(CR^1R^2)(OR)_2X_2$, in particular, were found to be only slightly active catalysts under normal conditions, despite their electronic and coordinatively unsaturated nature.[6,7] Their cationic derivatives $W(CR^1R^2)(OR)_2X^+$, on the other hand, are extremely active, which we proposed results mainly from the presence of a suitably positioned vacant site allowing olefin attack via Scheme Ia.[6-8]

Variable-temperature NMR studies were thus carried out to determine the rotational barriers in this family of neutral carbene complexes. For the compounds $W(CHR)(OCH_2\text{-}t\text{-}Bu)_2X_2$ (X = Cl, Br, I), no rotation of the carbene ligand could, however, be observed below the decomposition temperature (>150 °C for R = *t*-Bu) and only a minimum activation energy could thus be estimated for this process ($\Delta G^{\ddagger} > 23$ kcal·mol^{-1}, R = *t*-Bu). On substitution of the halide by neopentoxo ligands to form $W(CHR)(OCH_2\text{-}t\text{-}Bu)_3X$ (X = Cl, Br, I, OCH_2-*t*-Bu), the rotational barrier is markedly lowered and can be measured by NMR methods. During these studies a second dynamic process was discovered, which was also found to be intramolecular in nature.

In this paper, we thus discuss the detailed preparation of these new complexes, their ground-state structure as obtained from low temperature limiting ^{1}H NMR spectra, and their fluxional behavior in solution.

Results

Synthesis of $W(CR^1R^2)(OCH_2\text{-}t\text{-}Bu)_3X$ Complexes. The synthesis of $W(CH\text{-}t\text{-}Bu)(OCH_2\text{-}t\text{-}Bu)_2X_2$ [X = Cl, (**1**), Br (**2**), I (**3**)] and the general procedures enabling their conversion into $W(CR^1R^2)(OCH_2\text{-}t\text{-}Bu)_2X_2$ and $W(CR^1R^2)(OCH_2\text{-}t\text{-}Bu)_{2+n}X_{2-n}$ (n = 1, 2) have been reported in two preliminary communications.[6,9] They follow the five equations drawn out below.

$$WOCl_4 + 2\,t\text{-}BuCH_2OH \rightarrow WOCl_2(OCH_2\text{-}t\text{-}Bu)_2 + 2HCl$$

$$WOCl_2(OCH_2\text{-}t\text{-}Bu)_2 + Mg(CH_2\text{-}t\text{-}Bu)_2\cdot C_4H_8O_2 \rightarrow WO(CH_2\text{-}t\text{-}Bu)_2(OCH_2\text{-}t\text{-}Bu)_2 + MgCl_2\cdot C_4H_8O_2$$

$$WO(CH_2\text{-}t\text{-}Bu)_2(OCH_2\text{-}t\text{-}Bu)_2 + AlX_3 \rightarrow W(CH\text{-}t\text{-}Bu)(OCH_2\text{-}t\text{-}Bu)_2X_2 + CMe_4 + (AlOX)_n$$

The new air-sensitive complexes $W(CR^1R^2)(OCH_2\text{-}t\text{-}Bu)_2Br_2$ [R^1 = H, R_2 = *n*-Bu (**4**); R^1 = H, R^2 = *sec*-Bu (**5**); R^1 = H, R^2 = Ph (**6**); $CR^1R^2 = \overline{C(CH_2)_3CH_2}$ (**7**)] were prepared in methylene chloride from **2** and 15 equiv of 1-hexene, 3-methyl-1-pentene, styrene, and *exo*-methylenecyclopentane, respectively. This carbene exchange reaction is in fact followed by the slow catalytic

$$W(CH\text{-}t\text{-}Bu)(OCH_2\text{-}t\text{-}Bu)_2X_2 + CH_2{=}CR^1R^2 \rightarrow W(CR^1R^2)(OCH_2\text{-}t\text{-}Bu)_2X_2 + CH_2{=}CH\text{-}t\text{-}Bu$$

metathesis reaction of the olefins, the termination step of which causes progressive decomposition of the tungsten carbene complex catalyst. The reaction mixture has thus to be evaporated to remove olefin after a few hours, especially in the case of the most reactive compound **4**. The methylidene complex $W(CH_2)(OCH_2\text{-}t\text{-}Bu)_2Br_2$ has, however, not been isolated or even observed by in situ low-temperature NMR studies. Unlike compounds **1–3** which were obtained as orange oils, these four compounds are isolated as pale yellow (**4**), yellow-orange (**5**), or orange-red (**6**, **7**) solids.

Reaction of **1–7** with $Li(OCH_2\text{-}t\text{-}Bu)$ (1 equiv) in pentane yielded straightforwardly lithium halide and $W(CH\text{-}t\text{-}Bu)(OCH_2\text{-}t\text{-}Bu)_3X$ [X = Cl (**8**), Br (**9**), I (**10**)] and $W(CR^1R^2)(OCH_2\text{-}t\text{-}Bu)_3Br$ [R^1 = H, R^2 = *n*-Bu (**11**); R^1 = H, R^2 = *sec*-Bu (**12**); R^1 = H, R^2 = Ph (**13**); $CR^1R^2 = \overline{C(CH_2)_3CH_2}$ (**14**)], respectively, and addition of a second equivalent of neopentoxylithium to **9** gave $W(CH\text{-}t\text{-}Bu)(OCH_2\text{-}t\text{-}Bu)_4$ (**15**). No de-

$$W(CR^1R^2)(OCH_2\text{-}t\text{-}Bu)_2X_2 + n\text{Li}(OCH_2\text{-}t\text{-}Bu) \rightarrow W(CR^1R^2)(OCH_2\text{-}t\text{-}Bu)_{2+n}X_{2-n} + n\text{LiX}$$

protonation of the carbene ligand was observed in any of these reactions.[10] The tri- and tetraneopentoxo complexes **8–15** are again extremely soluble orange oils. The trineopentoxo compounds **8–14**, although quite stable in dilute solution, dismutate readily into the di- and tetraneopentoxo derivatives at high concentrations. Neither sublimation nor recrystallization or chromatography could thus be used as a purification method, and the complexes were studied after filtration of lithium halides without any further workup.

The cationic complex $[W(CH\text{-}t\text{-}Bu)(OCH_2\text{-}Bu)_3]^+Ga_2Br_7^-$ (**16**) was formed in situ by addition of an excess of gallium bromide to **9** at −35 °C. As reported previously[8] for $[W(CH\text{-}t\text{-}Bu)(OCH_2\text{-}t\text{-}Bu)_2Br]^+Ga_2Br_7^-$, it is unstable at room temperature and has not been isolated. Interestingly, the formation constant of **16** is, however, significantly superior to that of the above complex[8] and almost all **9** is converted into **16** after addition of only 2 equiv of $GaBr_3$.[7] Thus the π-donating alkoxo group appears to labilize the bromide ligand in the trans position.

Low Temperature Limiting ^{1}H NMR Spectra of Complexes $W(CR^1R^2)(OCH_2\text{-}t\text{-}Bu)_3X$. Low temperature limiting ^{1}H NMR spectra of all trineopentoxo complexes could be reached at 240 K in C_6D_5Br except for **8** which was obtained in $C_6D_5CD_3$ at 220

(6) Kress, J.; Wesolek, M.; Osborn, J. A. *J. Chem. Soc., Chem. Commun.* **1982**, 514.
(7) Kress, J.; Aguero, A.; Osborn, J. A. *J. Mol. Catal.* **1986**, *36*, 1.
(8) Kress, J.; Osborn, J. A. *J. Am. Chem. Soc.* **1983**, *105*, 6346.
(9) Aguero, A.; Kress, J.; Osborn, J. A. *J. Chem. Soc., Chem. Commun.* **1985**, 793.
(10) Freudenberger, J. H.; Schrock, R. R. *Organometallics* **1985**, *4*, 1937.

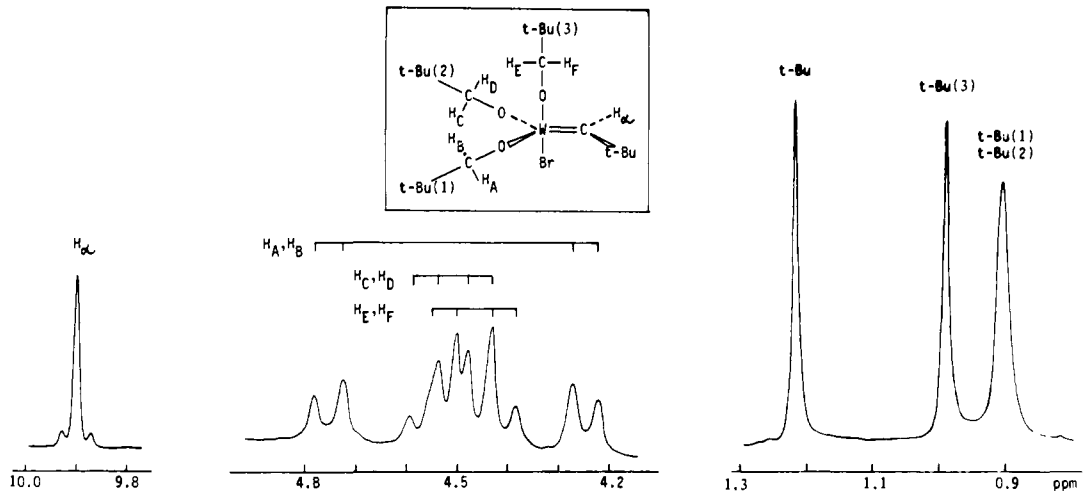

Figure 1. The ^{1}H NMR spectrum of W(CH-*t*-Bu)(OCH$_2$-*t*-Bu)$_3$Br (**9**) in C_6D_5Br at 235 K. (The 1.3–0.9-ppm range is reduced by a factor of 8.)

Table I. ^{1}H NMR Limiting Spectra of Complexes W(CR^{1}R^2)(OCH$_2$-*t*-Bu)$_3$X in C_6D_5Br at 240 K[a]

compound	H_α	R^1, R^2 ($\neq$H)	H_A, H_B	H_C, H_D	H_E,H_F	*t*-Bu(1),(2)	*t*-Bu(3)
W(CH-*t*-Bu)(OCH$_2$-*t*-Bu)$_3$Cl[b] (**8**)	9.61 (9.42)[c]	1.21 (1.22)[c]	4.78, 4.12	4.65, 4.32	4.59, 4.46	0.87, 0.82	1.02
W(CH-*t*-Bu)(OCH$_2$-*t*-Bu)$_3$Br (**9**)	9.90	1.23	4.75, 4.24	4.56, 4.46	4.52, 4.41	0.90 (0.86, 0.82)[b]	0.99
W(CH-*t*-Bu)(OCH$_2$-*t*-Bu)$_3$I (**10**)	10.19	1.25	4.75, 4.24	4.50	4.49, 4.40	0.91	0.99
W(CH-*n*-Bu)(OCH$_2$-*t*-Bu)$_3$Br (**11**)	10.32 (t)	4.89 (H_β), 1.32 (H_γ)	4.46, 4.27	4.46, 4.31	4.62	0.94	1.01
W(CH-*sec*-Bu)(OCH$_2$-*t*-Bu)$_3$Br (**12**)	10.13 (d) 10.10 (d)	4.44 (H_β), 1.36 (H_γ) 1.23 (Me_β), 1.10 (Me_γ)	4.52, 4.28	4.38	4.58	0.91	1.00
W(CHPh)(OCH$_2$-*t*-Bu)$_3$Br (**13**)	10.48	7.34–6.80	4.80, 4.36	4.62, 4.53	4.54, 4.47	0.95	0.89
W[C(CH$_2$)$_3$CH$_2$](OCH$_2$-*t*-Bu)$_3$Br (**14**)		5.86 (H_β), 1.33 (H_γ)	4.37, 4.25	4.34, 4.25	4.46	0.90	1.01
W(CH-*t*-Bu)(OCH$_2$-*t*-Bu)$_4$[d] (**15**)	8.01 (8.00)[c]	1.10	4.13	4.13	4.13	0.81	0.81
[W(CH-*t*-Bu)(OCH$_2$-*t*-Bu)$_3$]$^+$ (**16**)	11.93	1.02	5.02, 4.16	5.21, 4.48	5.28, 5.11	0.98	0.90

[a] δ in ppm/Me$_4$Si. $^2J_{^{183}WH}$ = 11–12 Hz. $^3J_{H_\alpha H_\beta}$ = 8–9 Hz. $^2J_{H_AH_B}$ = $^2J_{H_CH_D}$ = $^2J_{H_EH_F}$ = 12 Hz. H_A–H_F and *t*-Bu(1)–(3) refer to the assignments in Figure 1. [b] In tol-d_8, 220 K. [c] In C_6D_5Br at 240 K. [d] In CD_2Cl_2, 180 K. Limiting spectrum not observed.

K. For example, the spectrum of W(CH-*t*-Bu)(OCH$_2$-*t*-Bu)$_3$Br reported in Figure 1 thus shows the expected low-field singlet at 9.90 ppm (^{1}H) for the α proton of the neopentylidene ligand, with two satellites arising from its coupling with ^{183}W ($I = {}^1/_2$, 14.3% abundance, $^2J_{WH}$ = 12 Hz), as well as the corresponding *t*-Bu signal at 1.23 ppm (9 H). More interestingly, three AB quartets are found between 4.8 and 4.2 ppm (2 H each, $^2J_{HH}$ = 11.5 Hz) for the methylenic protons of the OCH$_2$-*t*-Bu groups. The two central quartets are partially superposed and coupling assignments were confirmed by selective decoupling experiments. These observations are in agreement (vide infra) with the presence of an idealized trigonal-bipyramidal (TBP) structure I in which the

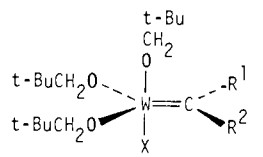

(I)

carbene ligand occupies an equatorial site with its two substituents lying in the trigonal plane of the TBP. The two equatorial and one axial neopentoxo groups are thus nonequivalent in **9** ($R^1 \neq R^2$), and each possess two diastereotopic $-CH_2-$ hydrogens. The assignment of H_A/H_B, H_C/H_D, and H_E/H_F shown in Figure 1 and Table I is based on symmetry considerations and on the effect of alkylidene and X substitution in **8–14** on the splitting and chemical shifts of the three quartets. The corresponding *t*-Bu signals at 0.99 (9 H) and 0.90 ppm (18 H) are assigned to the axial and the two equatorial neopentoxo groups, respectively, the latter being resolved into two singlets in deuteriotoluene at 220 K.

Among the other complexes possessing a neopentylidene ligand, **8** and **10** show similar spectra, the H_C and H_D protons being, however, accidently equivalent in **10** (Table I). The H_α signal is shifted to low field from **8** to **9** and from **9** to **10** and seems to depend on the π-donor strength of ligand X (Cl > Br > I), as already mentioned earlier.[7,9] The cationic complex **16** thus gives the lowest field resonance for H_α at 11.93 ppm and the tetraneopentoxo complex **15** the highest field resonance at 8.00 ppm. Three AB quartets are also observed for the OC*H*$_2$-*t*-Bu protons of complex [W(CH-*t*-Bu)(OCH$_2$-*t*-Bu)$_3$]$^+$ **16**, indicating a similar unsymmetrical structure for this cationic species. The four neopentoxo groups of compound W(CH-*t*-Bu)(OCH$_2$-*t*-Bu)$_4$ **15**, on the other hand, give rise to only one sharp singlet at 4.13 ppm (8 H), even at 180 K, indicating that the limiting spectrum is actually not reached in this case and that the molecule is still undergoing a fast dynamic exchange (vide infra).

The other =CHR alkylidene ligands bearing an α-hydrogen give rise as expected to a singlet in **13** (R = C_6H_5), a doublet in **12** (R = CHMeEt), and a triplet in **11** (R = CH_2Pr) for the H_α signal with $^3J_{H_\alpha H_\beta}$ = 8–9 Hz. The chemical shift progression toward low field **9** < **12** < **11** < **13** appears related to the decreasing σ-donor character of the R groups (*t*-Bu > *sec*-Bu > *n*-Bu > Ph).

For W(CH-*sec*-Bu)(OCH$_2$-*t*-Bu)$_3$Br (**12**), the H_α signal appears in fact as two doublets at 10.13 and 10.10 ppm (Table I), of approximately equal intensity. These correspond to the two diastereoisomers expected for a TBP molecule possessing two asymmetric centers, one at the tungsten and one at the β-carbon of the pentylidene ligand (cf. II).

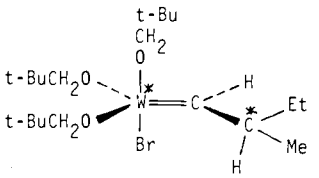

(II)

Table II. Coalescence Temperatures (T^C) and Average Activation Barriers ($\Delta G^\ddagger$) Observed for Compounds $W(CR^1R^2)(OCH_2\text{-}t\text{-}Bu)_3X$ in C_6D_5Br

compound	T^C_A (K) $H_AH_B + H_CH_D$	T^C_A (K) $H_E + H_F$	T^C_A (K) t-Bu(1) + t-Bu(2)	$\Delta G_A^\ddagger$ (kcal·mol^{-1})	T^C_B (K) $H_AH_BH_CH_D + H_EH_F$	T^C_B (K) t-Bu(1)-t-Bu(2) + t-Bu(3)	$\Delta G_B^\ddagger$ (kcal·mol^{-1})
$W(CH\text{-}t\text{-}Bu)(OCH_2\text{-}t\text{-}Bu)_3Cl$[a] (**8**)	245	245	235	12.3	380	370	18.9
$W(CH\text{-}t\text{-}Bu)(OCH_2\text{-}t\text{-}Bu)_3Br$ (**9**)	265	260	240	13.1	360	345	18.0
$W(CH\text{-}t\text{-}Bu)(OCH_2\text{-}t\text{-}Bu)_3I$ (**10**)	290	280	260	14.3	355	340	17.8
$W(CH\text{-}n\text{-}Bu)(OCH_2\text{-}t\text{-}Bu)_3Br$ (**11**)	290			15.7	320	310	15.9
$W(CH\text{-}sec\text{-}Bu)(OCH_2\text{-}t\text{-}Bu)_3Br$ (**12**)	285			14.4	335	325	16.9
$W(CHPh)(OCH_2\text{-}t\text{-}Bu)_3Br$ (**13**)	290	280		14.4	310	290	15.3
$W[\overline{C(CH_2)_3CH_2}](OCH_2\text{-}t\text{-}Bu)_3Br$ (**14**)					340	335	17.3
$W(CH\text{-}t\text{-}Bu)(OCH_2\text{-}t\text{-}Bu)_4$ (**15**)	<160			<8			
$[W(CH\text{-}t\text{-}Bu)(OCH_2\text{-}t\text{-}Bu)_3]^+$ (**16**)	>285	>285		>13.7	>285	>285	>13.7

[a] In tol-D_8.

The $OCH_2\text{-}t\text{-}Bu$ resonances of **11–14** are also consistent with structure I, assuming that accidental equivalence occurs for H_C and H_D in **12** and for H_E and H_F in **12** and **11**. For $W[\overline{C(CH_2)_3CH_2}](OCH_2\text{-}t\text{-}Bu)_3Br$ (**14**), the equivalence of H_A with H_D, H_B with H_C, and H_E with H_F results, however, clearly from the symmetrical nature of the cyclopentylidene ligand ($R^1 = R^2 = -CH_2CH_2-$) and from its coplanarity with the equatorial plane of the molecule (cf. I).

Although the low-temperature spectra are consistent with the TBP model proposed, a recent X-ray diffraction study[11] shows **7** to be dimeric in the solid state, two pentacoordinate approximately square pyramidal units weakly interacting via two long asymmetric tungsten halide interactions (**7a**). However, although

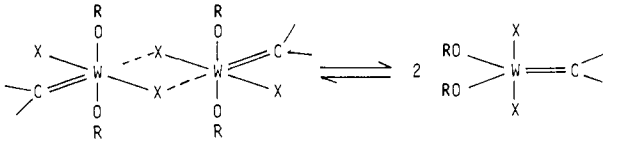

7a 7b

the other crystalline derivatives **4–6** are probably also dimers in the solid state, we believe that in solution they readily (and rapidly) dissociate into monomers as **7b**, as is evident from ^1H NMR studies.[11] We believe that the very pentane soluble oily materials **1–3** and **8–15** are also probably monomeric, although attempts to measure the molecular weight of these extremely air sensitive materials have been unsuccessful. The description of the momomeric species as TBP is certainly not totally exact, and deformation of these molecules toward a square-pyramidal form may well occur as found for dimeric **7a**, which is aided in this case, of course, by the presence of a weak interaction from a sixth ligand. The reader should thus bear in mind that the RO_{ax}–W–X angle in I may well be inferior to 180° and the equatorial O–W–O angle much greater than 120°. In any case, this would not substantially alter our qualitative discussion which follows.

Variable-Temperature ^1H NMR Studies. As the temperature of the C_6D_5Br solutions of compounds **8–13** is raised progressively, several reversible changes are observed in their ^1H NMR spectra.

For example, for the $OCH_2\text{-}t\text{-}Bu$ resonances of $W(CH\text{-}t\text{-}Bu)(OCH_2\text{-}t\text{-}Bu)_3Br$ (**9**, Figure 2), the AB quartets H_AH_B and H_CH_D coalesce to form a new AB quartet at 295 K [4.61 ppm (2 H), 4.33 ppm (2 H), $^2J_{HH}$ = 11.5 Hz], whereas the third AB quartet H_EH_F coalesces to a singlet at 4.44 ppm (2 H). Concomitantly, the signal arising from the two unresolved $OCH_2\text{-}t\text{-}Bu$ singlets [t-Bu(1) and t-Bu(2) in Figure 1] sharpens markedly, the coalescence probably occurring already at 240 K in this case. Note, however, that for **8** in toluene-d_8, the coalescence of the two $OCH_2\text{-}t\text{-}Bu$ peaks to a single resonance can be observed at 235 K, whereas the third t-Bu(3) signal is unaffected below 270 K (Figure 3). The values free energy of activation $\Delta G_A^\ddagger$ corresponding to these three distinct coalescence processes for **9** were calculated with use of the Eyring equation[12] (see Experimental Section) and were all equal within experimental error (13.1 ± 0.1 kcal·mol^{-1}, Table II), showing that these three spectral changes result almost certainly from one single temperature-dependent process, A.

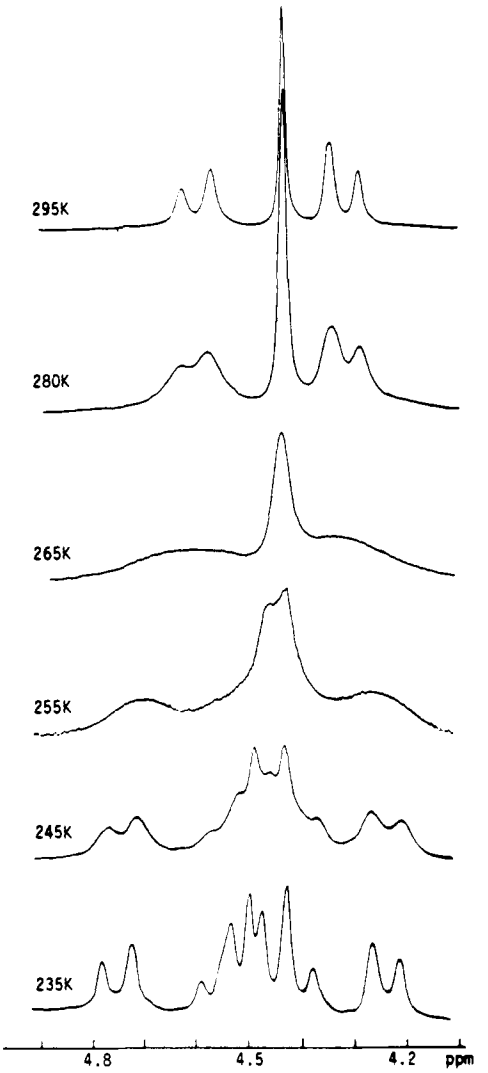

Figure 2. The $-OCH_2-$ NMR signals of $W(CH\text{-}t\text{-}Bu)(OCH_2\text{-}t\text{-}Bu)_3Br$ (**9**) in C_6D_5Br between 235 and 295 K.

At higher temperatures, the new AB quartet (corresponding to the four $H_AH_BH_CH_D$ protons) coalesces with the resonance

(11) Youinou, M. T.; Kress, J.; Fischer, J.; Aguero, A.; Osborn, J. A. *J. Am. Chem. Soc.*, submitted for publication.

(12) Gunther, H. *NMR Spektroskopie*; G. Thieme Verlag: Stuttgart, 1973.

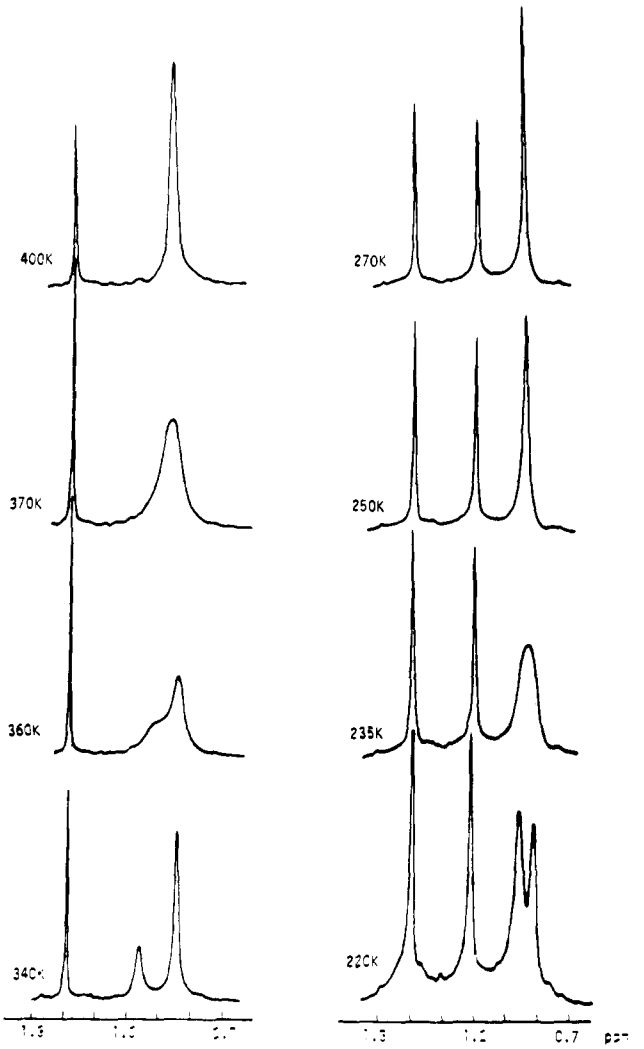

Figure 3. The *t*-Bu proton NMR signals of W(CH-*t*-Bu)(OCH_2-*t*-Bu)$_3$Cl (**8**) in tol-d_8 between 220 and 400 K.

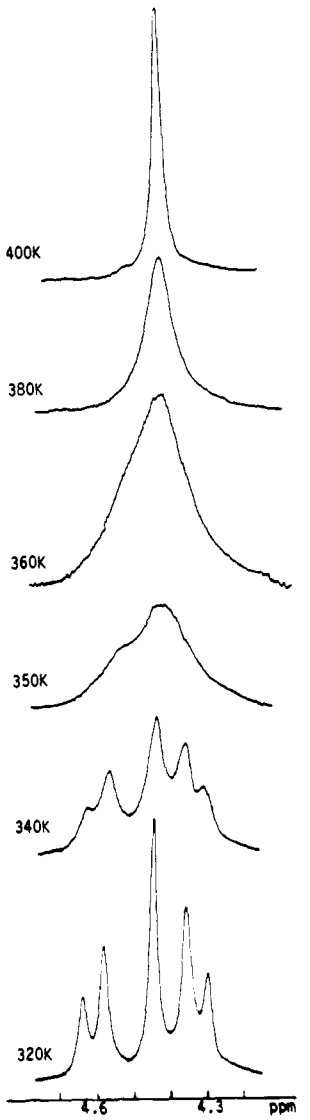

Figure 4. The $-OCH_2-$ NMR signals of W(CH-*t*-Bu)(OCH_2-*t*-Bu)$_3$Br (**9**) in C_6D_5Br between 320 and 400 K.

assigned to the two H_EH_F protons leading to a unique singlet at 4.43 ppm (6 H) at 400 K (Figure 4). Also the *t*-Bu(3) signal and the singlet arising from *t*-Bu(1) and *t*-Bu(2) coalesce to a single resonance at 0.92 ppm (27 H) at 400 K (Figure 3 for **8**). Again, the calculated activation barriers $\Delta G_B^{\ddagger} = 18.0 \pm 0.1$ kcal·mol^{-1} for these two coalescence processes were the same, indicating the existence of an additional temperature-dependent process, B.

Further, it was observed for both above dynamic processes A and B that the neopentylidene H_α and *t*-Bu (Figure 3) resonances remain unchanged and sharp and that the activation barriers are concentration independent, indicating their intramolecular nature. Further, the corresponding T^C and $\Delta G^{\ddagger}$ values are only slightly solvent dependent, appearing respectively 5–10 °C and ca. 0.5 kcal·mol^{-1} higher in toluene-d_8 than in bromobenzene-d_5.

Similar temperature-dependent spectra were observed for all neopentylidene complexes **8–10** as well as for the other alkylidene complexes **11–13**, the corresponding coalescence temperatures (T^C_A, T^C_B) and activation energies ($\Delta G_A^{\ddagger}$, $\Delta G_B^{\ddagger}$) of the two distinct processes being listed in Table II. However, the accidental equivalency of some of the protons occasionally allows for instance only one determination of $\Delta G_A^{\ddagger}$ (as in **11** and **12**), and the small energy difference existing in some cases between the two processes results in the partial superposition of the corresponding spectral changes (mainly for **11** and **13**). Therefore, the values reported in Table II for compounds **11–13** are somewhat less precise, especially for process A (±0.2 kcal·mol^{-1}).

For W(CH-*sec*-Bu)(OCH_2-*t*-Bu)$_3$Br (**12**), however, an additional observation can be made. The two alkylidene H_α doublets observed at 240 K (Table I) (which we have assigned to two distinct diastereoisomers) coalesce to a single doublet at 9.98 ppm at room temperature (T^C = 270 K). A $\Delta G^{\ddagger}$ value of 14.3 kcal·mol^{-1} was calculated for this process, indicating the equilibration of these H_α protons occurs during process A.

The three remaining complexes **14–16** listed in Table II show also certain particularities. For compound W[$\overline{C(CH_2)_3CH_2}$](OCH_2-*t*-Bu)$_3$Br (**14**) which possesses a plane of symmetry perpendicular to the equatorial plane of the molecule, the observation of the first process by following changes in the OCH_2-*t*-Bu resonances is now no longer possible although such a process must still be occurring. More importantly, the spectrum of W(CH-*t*-Bu)(OCH_2-*t*-Bu)$_4$ (**15**) remains unchanged from 180 K (Table I) to 400 K, showing throughout the same simple pattern as is found in the high temperature limiting spectra of complexes **8–10**. No coalescence data could thus be obtained in this case. If we assume that coalescence occurs below 160 K with an OCH_2-*t*-Bu peak separation of ca. 10 Hz in the hypothetical low temperature limiting spectrum, we can estimate a $\Delta G^{\ddagger}$ value inferior to 8 kcal·mol^{-1} (Table II). The cationic complex [W(CH-*t*-Bu)(OCH_2-*t*-Bu)$_3$]$^+$ (**16**), being unstable, could not be studied above 260 K, the temperature at which the three AB quartets due to the OCH_2-*t*-Bu protons are still sharp. Only a lower limit of $\Delta G^{\ddagger}$ = 13.7 kcal·mol^{-1} could thus be established in this case for either process A or process B (Table II). Much higher values are certainly involved.

The changes in spectra of an equimolecular mixture of W(CH-*t*-Bu)(OCH_2-*t*-Bu)$_3$Br (**9**) and W(CH-*t*-Bu)(OCH_2-*t*-Bu)$_3$I

(**10**) from room temperature to 380 K are identical with the superposition of the individual changes of each complex in agreement with the intramolecular nature of the process involved. In particular, the two H_α neopentylidene signals of **8** and **9** remain sharp. However, as the temperature is raised above 390 K, these two peaks begin to broaden and shift toward each other. Coalescence is not yet observed at 430 K, but it can be estimated to occur at ca. 450 K. A third dynamic process is thus occurring, the activation energy of which is estimated at $\Delta G^\ddagger$ = 22.5 kcal·mol^{-1}. In contrast to processes A and B, this process is intermolecular and involves undoubtedly halide exchange between monomeric units, via a dimeric halide bridged intermediate (see **7a**). We have not studied this process in further detail.

Discussion

Ground-State Structure. As already discussed, analysis of the low temperature limiting spectra of the complexes **8–14** allows us to propose the TBP (I) as the basic model for the ground-state structure of these species. Previous theoretical studies[13] have shown that the axial vs. equatorial preference of π-donor and acceptor ligands in a TBP structure is not clear-cut for a pentacoordinate d^2 complex (as W^{IV}, assuming carbene as a neutral π-acceptor ligand). However, should the equatorial site be occupied, the orientation of the carbene ligand parallel to the equatorial plane (IIIa) is preferred over the perpendicular form (IIIb) if the carbene is a weak π-acceptor. The important interaction in IIIa is that of the p_z orbital on the carbene with the d_{xz} orbital of the metal.

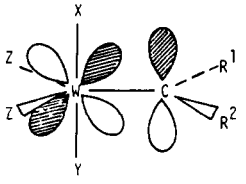

(IIIa)

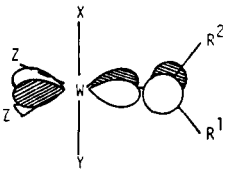

(IIIb)

An alternative but equivalent approach is to consider such complexes as W^{VI} (d^0), with the $(CR^1R^2)^{2-}$ as a strong π-donor ligand. This formalism allows the arrangement of ligands about W to be seen in terms of σ- and π-donor competition for the totally vacant metal orbital set and accounts in a simple fashion for the marked tendency shown by the most strongly π-donor ligands (RO > X) to occupy in preference the equatorial site in the series of complexes $W(CR^1R^2)(OCH_2\text{-}t\text{-}Bu)_2X_2$ and $W(CR^1R^2)(OCH_2\text{-}t\text{-}Bu)_3X$.[9,11]

Although we can readily understand structure I in terms of electronic effects we should note that the in-plane orientation of the carbene ligand probably also corresponds to the sterically most favored arrangement. However, as seen in arguments we develop later when discussing the effects of substituents on the carbene rotational barriers, a dominant role for electronic effects appears evident.

Process A. Carbene-Ligand Rotation about the Metal–Carbon Double Bond. Process A results in the equilibration of two equatorial neopentoxo ligands leaving the axial neopentoxo ligand distinct and in the equilibration of the two methylenic protons of the axial group leaving the corresponding equatorial protons distinct. This can be only reconciled with the occurrence of carbene-ligand rotation about the tungsten–carbon double bond (IIIa → IIIb). The loss of chirality at tungsten in **12** during this process is also consistent with this interpretation. A more refined description (i.e., involving concomitant bending modes of other ligands, for example, as in $Fe(CO)_4$(olefin)[14]) cannot as yet be offered but we note that such additional motions, should they occur, must not equilibrate axial with equatorial neopentoxo groups.

The trend in the values of $\Delta G_A^\ddagger$[15] for the corresponding rotational barriers of the various compounds (Table II) offers us some insight into the origin of this process. In a first stage, we note the following for complexes of formula $W(CH\text{-}t\text{-}Bu)(OCH_2\text{-}t\text{-}Bu)_2XY$: (a) when X = Y = halide (**1–3**), $\Delta G_A^\ddagger$ is large (>23 kcal·mol^{-1}); (b) when X = OCH_2-*t*-Bu, Y = halide (**8–10**), the values in $\Delta G_A^\ddagger$ decrease markedly and vary between 14.3 and 12.3 kcal·mol^{-1} in the order Y = I > Br > Cl (Table II, **10** > **9** > **8**; and (c) when X = Y = OCH_2-*t*-Bu (**15**), $\Delta G_A^\ddagger$ is very small (<8 kcal·mol^{-1}).

Replacement in axial site of a halide ligand by RO^- is thus shown to reduce greatly the rotational barrier. Clearly the presence of a stronger π-donor in axial site causes a four-electron destabilization interaction in IIIa, leaving IIIb largely unaffected. In the d^0 formalism, this interaction in IIIa can be seen to result

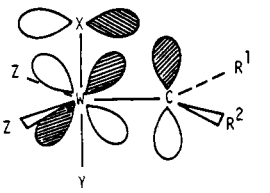

(IV)

from the competition created between the π-electrons of the axial alkoxo group and those of the carbene ligand (CR^1R^2) for the same vacant d_{xz} orbital of the tungsten (cf. IV). Hence, in either interpretation, the lowering of the rotational barrier of the carbene ligand results from this ground-state destabilization. Replacing a further axial halide ligand by RO^- increases this effect and should lower the rotational barrier even more. This is indeed observed, but the extremely low value estimated for $W(CH\text{-}t\text{-}Bu)(OCH_2\text{-}t\text{-}Bu)_4$ (**15**) might additionally result from the ground-state structure of this complex being now of a square pyramid (carbene apical), creating a more symmetric and lower fourfold barrier to rotation.

The decrease in $\Delta G_A^\ddagger$ observed for compounds $W(CH\text{-}t\text{-}Bu)(OCH_2\text{-}t\text{-}Bu)_3X$ in the order X = I (**10**) > Br (**9**) > Cl (**8**) can be similarly correlated with the increase in the π-donor nature of the halide ligands if we consider the π-donor order to be I < Br < Cl. This order although not conforming to that previously derived from spectroscopic measurements of low oxidation state complexes is indeed in agreement with our NMR and reactivity studies.[7,9] In the case where no ligand is present in the axial site, i.e., $W(CH\text{-}t\text{-}Bu)(OCH_2\text{-}t\text{-}Bu)_3^+$, the barrier might be expected to be even larger, although the instability of the cation allows only a lower limit of 13.7 kcal·mol^{-1} to be calculated from experimental data (but see below).

Furthermore, it appears for complexes of formula $W(CR^1R^2)(OCH_2\text{-}t\text{-}Bu)_3Br$ (**9**, **11–14**) that $\Delta G_A^\ddagger$ is also sensitive to the nature of the substituents on the carbene group and decreases in particular in the order R^2 (R^1 = H) = *n*-Bu (**11**) > *sec*-Bu (**12**) > *t*-Bu (**9**). As mentioned earlier, the ground-state TBP structure IIIa is sterically less crowded than the proposed intermediate IIIb, and thus steric destabilization of the ground state thereby lowering $\Delta G_A^\ddagger$ (as was found[5] in $TaCp_2(CHR)X$) in the order *t*-Bu > *sec*-Bu > *n*-Bu is unlikely here. We thus believe these trends in $\Delta G_A^\ddagger$ are again electronic in origin, the increasing σ-donor character of the R^2 groups increasing the negative charge on the carbene carbon, thereby increasing the destabilizing interaction with the axial electrons. Interestingly, we have observed a correlation between $\Delta G_A^\ddagger$ values and the corresponding H_α chemical shifts of the various compounds (Figure 5A), depending on changes in σ-donor groups R^1,R^2 (line ii) or π-donor ligands (line i). We have not attempted to interpret such a relation further (the interpretation of chemical shift data alone presents difficulties), but we note that using the H_α shift for $W(CH\text{-}t\text{-}Bu)(OCH_2\text{-}t\text{-}Bu)_3^+$ we can estimate a $\Delta G_A^\ddagger$ for this

(13) Rossi, A. R.; Hoffmann, R. *Inorg. Chem.* **1975**, *14*, 365.
(14) Wilson, S. T.; Coville, N. J.; Shapley, J. R.; Osborn, J. A. *J. Am. Chem. Soc.* **1974**, *96*, 4038.

(15) Several calculations have been carried out on the rotational barriers for d^2 carbene systems, and values 0–37 kcal·mol^{-1} (Ti^{II}),[7k] 10.4 kcal·mol^{-1} (Ti^{II}),[7j] 11.3 kcal·mol^{-1} (Nb^{III}),[7i] 14.6 kcal·mol^{-1} (Nb^{III}),[7h] and 30.6 and 23.1 kcal·mol^{-1} (Mo^{IV})[7e] have been obtained.

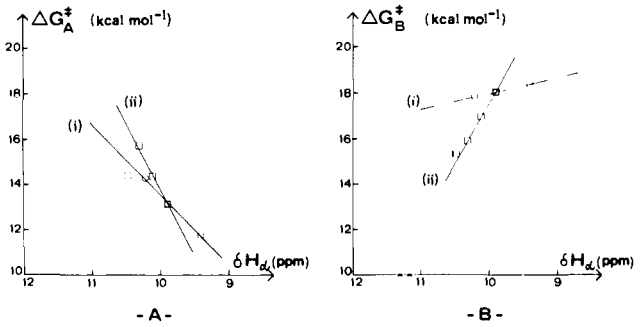

Figure 5. $\Delta G^{\ddagger}$ values (Table II) vs. H_α chemical shifts (Table I) for compounds $W(CHR)(OCH_2\text{-}t\text{-}Bu)_3X$ (**8–13**): (A) line (i), $\Delta G_A^{\ddagger}$ for R = *t*-Bu, X = Cl*, Br, I, and line (ii), $\Delta G_A^{\ddagger}$ for R = *t*-Bu, *sec*-Bu, *n*-Bu, Ph, X = Br; (B) line (i), $\Delta G_B^{\ddagger}$ for R = *t*-Bu, X = Cl*, Br, I, and line (ii), $\Delta G_B^{\ddagger}$ for R = *t*-Bu, *sec*-Bu, *n*-Bu, Ph, X = Br. For the compound with an asterisk, the $\Delta G^{\ddagger}$ values reported in Table II were corrected by the difference of 0.5 kcal·mol^{-1} existing between toluene and bromobenzene solvents.

species as ca. as 20 kcal·mol^{-1}. However, note that the H_α shift (10.87 ppm) for $W(CH\text{-}t\text{-}Bu)(OCH_2\text{-}t\text{-}Bu)_2Cl_2$, for example, would predict a value of $\Delta G_A^{\ddagger}$ of 16 kcal·mol^{-1}, much lower than the minimum value (23 kcal·mol^{-1}) calculated for this compound from spectroscopic data. Hence either this correlation is unreliable or, alternatively, other effects such as structural changes are occurring when a neopentoxo group replaces a halide in an axial site.

Process B. Intramolecular Ligand Exchange. The "high-energy" process B in the complexes $W(CR^1R^2)(OCH_2\text{-}t\text{-}Bu)_3X$ causes all three neopentoxo groups to equilibrate intramolecularly, as well as all methylenic protons. $\Delta G_B^{\ddagger}$ for this process appears to be in all cases superior to $\Delta G_A^{\ddagger}$ (Table II). However, we cannot assert whether or not prior carbene rotation is necessary for process B to take place.

Process B is not, however, particular to carbene complexes. We have observed similar equilibration phenomena for neopentoxo groups in $WO(OCH_2\text{-}t\text{-}Bu)_3(CH_2\text{-}t\text{-}Bu)$ ($\Delta G^{\ddagger}$ = 13.2 kcal·mol^{-1})[16] and for the neopentyl ligands in $WO(CH_2\text{-}t\text{-}Bu)_3(NR_2)$ ($\Delta G^{\ddagger}$ = 18–20 kcal·mol^{-1} depending on R).[17]

We do not at present propose a detailed mechanism for these rearrangements. Pentacoordination is notorious for its structural flexibility, although studies have largely concentrated on group V species and d^8 transition-metal complexes. Early transition metal complexes have received little attention, but we note that invoking a series of stepwise intramolecular exchange processes of the Berry pseudorotation type is somewhat complicated and extremely cumbersome in the present case.

The dependence of $\Delta G_B^{\ddagger}$ (Table II) on π-donor substitution in an axial site is in the opposite sense to $\Delta G_A^{\ddagger}$, the barrier increasing in the order I < Br < Cl. Similarly the trend in substituent changes on the carbene ligand is reversed from $\Delta G_A^{\ddagger}$ to $\Delta G_B^{\ddagger}$. Steric effects may be involved in process B. However, $\Delta G_B^{\ddagger}$ can again be correlated with chemical shift data of H_α (Figure 5B); with use of line i and H_α position for **16** a $\Delta G_B^{\ddagger}$ value can be calculated as ca. 17 kcal·mol^{-1}, which is less than $\Delta G_A^{\ddagger}$. Unfortunately since experimental data for **16** cannot be obtained, we are unable to confirm if process B can or cannot occur without prior carbene rotation in these systems.

Conclusion

We have shown that the rotational barriers about the metal–carbon double bond in a family of metal–carbene complexes are dependent both on the π-donor nature of the ligands and on σ-effects of the substituent groups on the carbene itself.

However, we find that the ease of rotation of the carbene group follows these ligand effects in the opposite sense to that we have observed for the activity of such complexes as olefin metathesis catalysts.[7] It would thus seem safe to conclude that carbene rotation even if present at some stage in the catalytic cycle probably is not implicated in the rate-determining step for these complexes.

Experimental Section

All manipulations were carried out in a N_2-filled Vacuum Atmospheres drybox equipped with a purification train HE-493, or with use of standard Schlenk or vacuum line techniques.

1-Hexene, 3-methyl-1-pentene, and *exo*-methylenecyclopentane were purchased from Aldrich, refluxed over a sodium–paraffin dispersion, and distilled trap to trap under vacuum. Reagent grade styrene (Aldrich) was used without further purification. Dichloromethane (Merck) was dried over aluminum chloride and distilled under nitrogen. Pentane and hexane were dried over sodium–benzophenone ketyl and distilled under nitrogen. Neopentoxylithium was prepared in hexane from n-butyllithium and neopentanol (Aldrich) and recrystallized from hexane. Gallium bromide was purchased from Ventron and sublimed under vacuum. Bromobenzene-d_5, toluene-d_8, dichloromethane-d_2, and benzene-d_6 were purchased from C.E.A.

^1H and ^{13}C NMR spectra were run at respectively 200.13 and 50.33 MHz on a Bruker SY 200 spectrometer equipped with a B-VT 1000 variable-temperature set.

Chemical shift calibration was based on solvent peaks at (^1H) 7.28, 5.33, 2.03, and 7.27 ppm or at (^{13}C) 122.1, 53.6, 21.2, and 128.0 ppm for respectively bromobenzene, dichloromethane, toluene, and benzene.

Infrared spectra were recorded on a Perkin-Elmer 597 spectrometer with cesium iodide disks.

Preparation of $W(CH\text{-}n\text{-}Bu)(OCH_2\text{-}t\text{-}Bu)_2Br_2$. To an orange solution of 260 mg of $W(CH\text{-}t\text{-}Bu)(OCH_2\text{-}t\text{-}Bu)_2Br_2$[6] (0.44 mmol) in dichloromethane (15 mL) was added 0.83 mL of 1-hexene (6.64 mmol). After 2 h, the reaction mixture had become darker, the volatiles were removed in vacuo, and the brown residue was washed three times with pentane to give 180 mg (69%) of product as a pale yellow, extremely air-sensitive, powder. Recrystallization from pentane gives light-orange crystals.

^1H NMR (CD_2Cl_2): δ (ppm) 11.65 (t, 1 H, $^3J_{HH}$ = 7.5 Hz, W=C*H*–), 4.86 (dt, 2 H, $^3J_{HH}$ = 7.5 and 7 Hz, =CHCH_2–), 4.32 (s, 4 H, –OCH_2–), 1.44 (m, 4 H, –CH_2(CH_2)$_2CH_3$), 1.01 and 1.00 (s, 9 H, –OCH_2-*t*-*Bu*), 0.94 (t, 3 H, $^3J_{HH}$ = 7 Hz, –CH_2CH_3).

^{13}C NMR (C_6D_6, gated decoupled): δ (ppm) 292.9 (very broad, W=*C*H), 91.0 and 90.6 (t, –*O*CH_2–), 43.8 (t, =CH*C*H_2–), 35.1 (t, –*C*$H_2CH_2CH_3$), 34.4 and 33.9 (s, OCH_2*C*Me_3), 26.5 and 26.4 (q, OCH_2C*Me*$_3$), 22.6 (t, –CH_2*C*H_2CH_3), 13.9 (q, –CH_2*C*H_3).

IR (Nujol mull): $\nu_{W=O}$ 700 cm^{-1} (strong), $\nu_{W\text{-}Br}$ (>200 cm^{-1}) 205 cm^{-1} (medium).

Preparation of $W(CH\text{-}sec\text{-}Bu)(OCH_2\text{-}t\text{-}Bu)_2Br_2$. To an orange solution of 283 mg of $W(CH\text{-}t\text{-}Bu)(OCH_2\text{-}t\text{-}Bu)_2Br_2$[6] (0.48 mmol) in dichloromethane (15 mL) was added 0.91 mL of 3-methyl-1-pentene (7.22 mmol). After 4 h and a slight darkening of the reaction mixture, volatiles were removed in vacuo and the orange-brown residue was washed two times with 0.5 mL of pentane to yield 210 mg (74%) of product as a pale orange powder which can be recrystallized from pentane. This compound is quite soluble in pentane and its washing has to be carried out with as little pentane as possible.

^1H NMR (C_6D_6): δ (ppm) 11.40 (d, 1 H, $^3J_{HH}$ = 9.5 Hz, W=C*H*–), 4.58 (m, 1 H, =CHC*H*<), 4.41 and 4.39 (s, 2 H, –OCH_2–), 1.41 (m, 2 H, –CHCH_2CH$_3$), 1.24 (d, 3 H, $^3J_{HH}$ = 6.5 Hz, –CHCH_3), 1.13 (t, 3 H, $^3J_{HH}$ = 7 Hz, –CH_2CH_3), 1.00 and 0.99 (s, 9 H, –OCH_2-*t*-*Bu*).

^{13}C NMR (C_6D_6, gated decoupled) δ (ppm) 296.1 (d, br, $^1J_{CH}$ = 138 Hz, W=*C*H–), 91.1 and 90.7 (t, $^1J_{CH}$ = 150 Hz, –*O*CH_2), 50.9 (d, $^1J_{CH}$ = 131 Hz, =CH*C*H), 34.4 and 34.0 (s, OCH_2*C*Me_3), 34.2 (t, $^1J_{CH}$ = 125 Hz, –CH*C*H_2CH_3), 26.5 and 26.4 (q, $^1J_{CH}$ = 125 Hz, –OCH_2C*Me*$_3$), 22.4 (q, $^1J_{CH}$ = 123 Hz, –CH*C*H_3), 12.7 (q, $^1J_{CH}$ = 122 Hz, –CH_2*C*H_3).

IR (Nujol mull): $\nu_{W=O}$ 700 cm^{-1} (strong), $\nu_{W\text{-}Br}$ (>200 cm^{-1}) 205 cm^{-1} (medium).

Preparation of $W(CHPh)(OCH_2\text{-}t\text{-}Bu)_2Br_2$. To an orange solution of 282 mg of $W(CH\text{-}t\text{-}Bu)(OCH_2\text{-}t\text{-}Bu)_2Br_2$[6] (0.48 mmol) in dichloromethane (15 mL) was added 0.82 mL of styrene (7.13 mmol). After 4 h, the volatiles of the red reaction mixture were removed in vacuo and the orange-red residue was washed two times with pentane to yield 270 mg (92%) of product as an orange-red powder. Recrystallization from pentane gives red crystals.

^1H NMR (C_6D_6): δ (ppm) 11.67 (s, 1 H, W=C*H*–), 7.33–6.80 (5 H, Ph), 4.55 and 4.52 (s, 2 H, –OCH_2–), 1.03 and 0.99 (s, 9 H, –OCH_2-*t*-*Bu*).

^{13}C NMR (C_6D_6, gated decoupled): δ (ppm) 279.6 (d, br, $^1J_{CH}$ = 141 Hz, W=*C*H–), 139.2 (s, C_1 on Ph), 132.1 (d, $^1J_{CH}$ = 160 Hz, C_2 and C_6 on Ph), 130.6 (d, $^1J_{CH}$ = 158 Hz, C_3 and C_5 on Ph), 127.4 (d, $^1J_{CH}$ = 156 Hz, C_4 on Ph), 92.6 and 91.4 (t, $^1J_{CH}$ = 149 Hz, –*O*CH_2), 34.5

(16) Unpublished results.
(17) Le Ny, J. P. Thesis, 1984, ULP Strasbourg.

and 34.2 (s, $-OCH_2CMe_3$), 26.5 (q, $^1J_{CH}$ = 127 Hz, $-OCH_2CMe_3$).

Preparation of W[C(CH$_2$)$_3$CH$_2$](OCH$_2$-*t*-Bu)$_2$Br$_2$. To an orange solution of 127 mg of W(CH-*t*-Bu)(OCH$_2$-*t*-Bu)$_2$Br$_2$[6] (0.215 mmol) in dichloromethane (10 mL) was added 0.36 mL of *exo*-methylenecyclopentane (3.42 mmol). After 4 h, the volatiles of the red reaction mixture were removed in vacuo and the orange residue was washed two times with pentane to give 110 mg (87%) of product as an orange powder. Recrystallization from pentane gives red crystals.

^{1}H NMR (C_6D_6): δ (ppm) 5.84 (m, 4 H, W=CC*H*$_2$–), 4.41 (s, 4 H, –OC*H*$_2$–), 1.29 (m, 4 H, =CCH$_2$C*H*$_2$–), 1.01 (s, 18 H, –OCH$_2$-*t*-*Bu*).

^{13}C NMR (CD_2Cl_2, gated decoupled): δ (ppm) 90.2 (t, $^1J_{CH}$ = 149 Hz, –*O*CH$_2$–), 47.1 (t, $^1J_{CH}$ = 134 Hz, W=*C*CH$_2$–), 34.1 (s, OCH$_2$*C*Me$_3$), 28.2 (t, $^1J_{CH}$ = 131 Hz, =CCH$_2$*C*H$_2$–), 26.4 (q, $^1J_{CH}$ = 127 Hz, $-OCH_2CMe_3$). The W=*C* signal was not observed. It appears, however, as a singlet at 335.7 ppm in the spectrum of the gallium bromide adduct (220 K).

IR (Nujol mull): ν_{W-O} 700 cm^{-1} (strong), ν_{W-Br} (>200 cm^{-1}) 205 cm^{-1} (medium).

IR (cyclohexane): ν_{W-O} 700 cm^{-1} (strong) and 665 cm^{-1} (medium).

Preparation of W(CH-*t*-Bu)(OCH$_2$-*t*-Bu)$_3$Cl. A solution of 27 mg of LiOCH$_2$-*t*-Bu (0.29 mmol) in 5 mL of pentane was added dropwise to 118 mg of W(CH-*t*-Bu)(OCH$_2$-*t*-Bu)$_2$Cl$_2$[6] (0.24 mmol) in pentane (5 mL) causing no apparent color change. Volatiles were removed under vacuum, and the residue was retreated with pentane. Slowly LiCl began to precipitate from the orange solution as a white powder. This was filtered off and the pentane removed under vacuum to give 127 mg (98%) of product as an orange extremely pentane soluble oil. This could not be crystallized, and its short path distillation at 70 °C under vacuum yielded mainly W(CH-*t*-Bu)(OCH$_2$-*t*-Bu)$_2$Cl$_2$. Although a satisfactory degree of purity could be obtained according to the ^{1}H NMR spectra, impurities identified as the tungsten alkyl compounds WO(OCH$_2$-*t*-Bu)$_3$(CH$_2$-*t*-Bu) and W(OCH$_2$-*t*-Bu)$_4$(CH$_2$-*t*-Bu)Cl[16] were frequently present which result from a complex protonation reaction of the carbene ligand. These observations are somewhat surprising since one would rather expect deprotonation to occur to produce a carbyne complex.[10]

^{1}H NMR: cf. Table I. Irradiation of the doublets at 4.78, 4.65, or 4.59 ppm causes the doublets at resepctively 4.12, 4.32, or 4.46 ppm to become singlets, and reciprocally.

^{13}C NMR (C_6D_6, ^{1}H decoupled, room temperature): δ (ppm) 269.4 (W=*C*H), 94.2 (–O*C*H$_2$– ax), 88.5 (–O*C*H$_2$– eq), 34.7 (=*C*CMe$_3$), 26.8 (OCH$_2$C*Me*$_3$ ax), 26.5 (OCH$_2$C*Me*$_3$ eq).

Preparation of W(CH-*t*-Bu)(OCH$_2$-*t*-Bu)$_3$X (X = Br, I). The procedures and yields for the reaction of W(CH-*t*-Bu)(OCH$_2$-*t*-Bu)$_2$X$_2$ (X = Br, I) with 1 equiv of LiONp were similar to those described for the chlorinated derivative, as are the properties of the orange products. LiI, however, always precipitated instantaneously.

^{1}H NMR: cf. Table I and Figure 1.

^{13}C NMR (X = Br) (C_6D_5Br, gated decoupled, room temperature): δ (ppm) 273.7 (d, $^1J_{WC}$ = 182 Hz, $^1J_{CH}$ = 135 Hz, W=*C*H), 93.8 (t, $^1J_{CH}$ = 142 Hz, –O*C*H$_2$– ax), 89.0 (t, $^1J_{CH}$ = 146 Hz, –O*C*H$_2$– eq), 43.5 (s, =CH*C*Me$_3$), 34.9 (s, OCH$_2$*C*Me$_3$ ax), 34.1 (q, $^1J_{CH}$ = 126 Hz, =CHC*Me*$_3$), 33.6 (s, OCH$_2$*C*Me$_3$ eq), 26.5 (q, $^1J_{CH}$ = 123 Hz, OCH$_2$C*Me*$_3$ ax), 26.3 (q, $^1J_{CH}$ = 125 Hz, OCH$_2$C*Me*$_3$ eq).

^{13}C NMR (X = I) (C_6D_6, ^{1}H decoupled, room temperature): δ (ppm) 279.6 ($^1J_{WC}$ = 182 Hz, W=*C*H), 93.9 (–O*C*H$_2$– ax), 91.4 (br, –O*C*H$_2$– eq), 44.7 (=CH*C*Me$_3$), 34.2 (=CHC*Me*$_3$), 26.8 (OCH$_2$C*Me*$_3$ ax), 26.6 (OCH$_2$C*Me*$_3$ eq).

Preparation of W(CR^{1}R^2)(OCH$_2$-*t*-Bu)$_3$Br [R^1 = H, R^2 = *n*-Bu, *sec*-Bu, or Ph; CR^{1}R^2 = C(CH$_2$)$_3$CH$_2$]. These compounds were obtained as described previously by the reactions of complexes W(CH-*n*-Bu)(OCH$_2$-*t*-Bu)$_2$Br$_2$, W(CH-*sec*-Bu)(OCH$_2$-*t*-Bu)$_2$Br$_2$, W(CHPh)(OCH$_2$-*t*-Bu)$_2$Br$_2$, and W[C(CH$_2$)$_3$CH$_2$](OCH$_2$-*t*-Bu)$_2$Br$_2$ with 1 equiv LiONp. All products were unstable in concentrated solution and were highly pentane soluble orange-brown oils. The two corresponding alkyl compounds were also occasionally detected as impurities.

^{1}H NMR: cf. Table I.

Preparation of W(CH-*t*-Bu)(OCH$_2$-*t*-Bu)$_4$. A solution of 54 mg of LiOCH$_2$-*t*-Bu (0.58 mmol) in 5 mL of pentane was added dropwise to 158 mg of W(CH-*t*-Bu)(OCH$_2$-*t*-Bu)$_2$Br$_2$[6] (0.27 mmol) in pentane (5 mL). LiBr precipitated after a few minutes as a white powder and was separated by filtration. Pentane was removed from the orange solution under vacuum to give 136 mg (84%) of product as an orange extremely pentane soluble oil. Contamination with small quantities of WO(OCH$_2$-*t*-Bu)$_3$(CH$_2$-*t*-Bu) was usually observed.

^{1}H NMR: cf. Table I.

^{13}C NMR (C_6D_6, gated decoupled, room temperature): δ (ppm) 252.6 (d, $^1J_{WC}$ = 192 Hz, $^1J_{CH}$ = 137 Hz, W=*C*H), 88.6 (t, $^1J_{CH}$ = 141 Hz, –O*C*H$_2$–), 41.8 (s, =CH*C*Me$_3$), 34.7 (s, OCH$_2$*C*Me$_3$), 36.4 (q, $^1J_{CH}$ = 124 Hz, =CHC*Me*$_3$), 26.8 (q, $^1J_{CH}$ = 124 Hz, OCH$_2$C*Me*$_3$).

Formation of [W(CH-*t*-Bu)(OCH$_2$-*t*-Bu)$_3$]$^+$ Ga$_2$Br$_7^-$. Finely ground gallium bromide (32 mg, 0.103 mmol) was introduced at the top of an ^{1}H NMR tube containing 10 mg of W(CH-*t*-Bu)(OCH$_2$-*t*-Bu)$_3$Br (0.017 mmol) in C_6D_5Br (0.45 mL). The NMR tube was cooled to –80 °C and then shaken vigorously and allowed to warm up just enough to allow complete dissolution of the gallium bromide. The reaction mixture was then quickly cooled again to –80 °C and later analyzed by NMR at –35 °C. The displacement of the equilibrium W(CH-*t*-Bu)(OCH$_2$-*t*-Bu)$_3$Br·GaBr$_3$ + GaBr$_3$ ⇌ [W(CH-*t*-Bu)(OCH$_2$-*t*-Bu)$_3$]$^+$Ga$_2$Br$_7^-$ to the right was checked by analyzing the NMR spectra of several solutions containing various amounts of GaBr$_3$ ($1 < n$ equiv < 6), which allowed us to calculate an equilibrium constant of ca. 600 M^{-1} at 240 K.[7,8]

^{1}H NMR: cf. Table I. Irradiation of the doublets at 4.16, 4.48, or 5.11 ppm causes the doublets at respectively 5.02, 5.21, or 5.28 ppm to become singlets. On raising the temperature decomposition begins to occur at 250 K, but there was sufficient compound remaining at 260 K to show that absolutely no broadening of the signals is observed at this temperature.

Variable-Temperature Studies. The ^{1}H NMR spectra of the various fluxional compounds were run at ca. 15 different temperatures in the concentration range $5–7 \times 10^{-2}$ M. Concentration effects were analyzed on W(CH-*t*-Bu)(OCH$_2$-*t*-Bu)$_3$Cl (low-temperature process) and W(CH-*t*-Bu)(OCH$_2$-*t*-Bu)$_3$Br (high-temperature process) by diluting solutions over a factor of 4. Solvent effects (bromobenzene, toluene) were analyzed with W(CH-*t*-Bu)(OCH$_2$-*t*-Bu)$_3$Br (low-temperature process) and W(CH-*t*-Bu)(OCH$_2$-*t*-Bu)$_3$Cl or W(CH-*n*-Bu)(OCH$_2$-*t*-Bu)$_3$Br (high-temperature process).

The 1/1 mixture of W(CH-*t*-Bu)(OCH$_2$-*t*-Bu)$_3$Br and W(CH-*t*-Bu)(OCH$_2$-*t*-Bu)$_3$I in bromobenzene on which the intermolecular halide exchange was studied had a total concentration of 6×10^{-2} M.

Calculations of $\Delta G^{\ddagger}$. The $\Delta G^{\ddagger}$ values were calculated with the Eyring equation[12] $\Delta G^{\ddagger} = 4.57T^{C}(9.97 + \log T^{C}/\Delta\nu)$ cal·mol^{-1} where T^{C}(K) is the temperature of coalescence of two given signals and $\Delta\nu$(Hz) their difference in chemical shift. The $\Delta G^{\ddagger}$ of the low-energy process of W(CH-*t*-Bu)(OCH$_2$-*t*-Bu)$_3$Br were found to be equal to (a) 13.1 kcal·mol^{-1} from the coalescence of the two AB quartets assigned to H_AH_B and H_CH_D into a single quartet, (b) 13.1 kcal·mol^{-1} from the coalescence of the AB quartet assigned to H_EH_F into a singlet, and (c) 13.0 kcal·mol^{-1} from the coalescence of the two singlets assigned to the *t*-Bu groups of the two equatorial OCH$_2$-*t*-Bu ligands into a single resonance. For the high-energy process of the same compound, we found 18.0 and 17.9 kcal·mol^{-1} from respectively the O*CH*$_2$-*t*-Bu and OCH$_2$-*t*-*Bu* spectra. The error on the average values of 13.1 and 18.0 kcal·mol^{-1} reported in Table II for the two dynamic processes can thus be estimated at ±0.1 kcal·mol^{-1}.

Values of $\Delta G^{\ddagger}$ for other compounds were obtained similarly.